



OPEN

SUBJECT AREAS:

MARINE CHEMISTRY
CLIMATE-CHANGE IMPACTS

PALAEOCLIMATE

Received
2 October 2013Accepted
7 May 2014Published
3 June 2014

Correspondence and
requests for materials
should be addressed to
Y.L. (gee@ustc.edu.
cn); C.-F.Y. (cfy20@
mail.ncku.edu.tw) or
C.-C.S. (river@ntu.edu.
tw)

Acceleration of modern acidification in the South China Sea driven by anthropogenic CO₂

Yi Liu^{1,2}, Zicheng Peng¹, Renjun Zhou^{1,3}, Shaohua Song², Weiguo Liu², Chen-Feng You⁴, Yen-Po Lin⁴, Kefu Yu⁵, Chung-Che Wu⁶, Gangjian Wei⁷, Luhua Xie⁷, George S. Burr⁶ & Chuan-Chou Shen⁶

¹CAS Key Laboratory of Crust-Mantle Material and Environment, School of Earth and Space Science, University of Science and Technology of China, Hefei 230026, China, ²State Key Laboratory of Loess and Quaternary Geology, Institute of Earth Environment, Chinese Academy of Sciences, Xi'an 710075, China, ³CAS Key Laboratory of Geospace Environment, School of Earth and Space Sciences, University of Science and Technology of China, Hefei 230026, China, ⁴Earth Dynamic System Research Center (EDSRC), National Cheng Kung University, Tainan 701, Taiwan, ⁵South China Sea Institute of Oceanology, Chinese Academy of Sciences, Guangzhou 510301, China, ⁶High-Precision Mass Spectrometry and Environment Change Laboratory (HISPEC), Department of Geosciences, National Taiwan University, Taipei 10617, Taiwan, ⁷State Key Laboratory of Isotope Geochronology and Geochemistry, Guangzhou Institute of Geochemistry, Chinese Academy of Sciences, Guangzhou 510640, China.

Modern acidification by the uptake of anthropogenic CO₂ can profoundly affect the physiology of marine organisms and the structure of ocean ecosystems. Centennial-scale global and regional influences of anthropogenic CO₂ remain largely unknown due to limited instrumental pH records. Here we present coral boron isotope-inferred pH records for two periods from the South China Sea: AD 1048–1079 and AD 1838–2001. There are no significant pH differences between the first period at the Medieval Warm Period and AD 1830–1870. However, we find anomalous and unprecedented acidification during the 20th century, pacing the observed increase in atmospheric CO₂. Moreover, pH value also varies in phase with inter-decadal changes in Asian Winter Monsoon intensity. As the level of atmospheric CO₂ keeps rising, the coupling global warming via weakening the winter monsoon intensity could exacerbate acidification of the South China Sea and threaten this expansive shallow water marine ecosystem.

The present-day level of atmospheric CO₂ is the highest known to occur for the past 2 million years¹. One half of the total modern anthropogenic CO₂ emissions have been absorbed by the ocean with an estimated rate of up to 1 million metric tons per hour^{2,3}, resulting in a reduction of seawater pH (pH_{sw}) and so-called ocean acidification. Sea surface pH_{sw} dropped by ~0.1 unit relative to preindustrial time, based on modeling estimates⁴ and is projected to decrease by another 0.3–0.4 units by AD 2100 under the IS92a “business-as-usual” scenario⁵. Ocean acidification could lead to significant shifts in the structure and dynamics of ocean ecosystems. One of the direct impacts of acidification is that it may lead to a decrease in the saturation state of surface ocean waters with respect to CaCO₃. This is a threat to marine organisms that rely on the process of calcification to construct their skeletons^{6–8}. These studies are based on modern observations and model predictions⁴ with a pH_{sw} decrease rate of ~0.002 year^{−1} (ref. 5). However, instrumental pH_{sw} records are sparse and span no more than three decades^{9,10}. Natural archives offer an alternative approach to reconstruct pre-instrumental pH_{sw} records much further back in time.

Biogenic carbonate δ¹¹B data have been suggested as a promising proxy to reconstruct ambient pH_{sw} since the 1990s (refs. 11,12). Recent studies^{13–15} showed that coral δ¹¹B could faithfully record pH values of extracellular calcifying fluids (pH_{cf}) that depend directly on ambient (external) seawater pH_{sw}. Only two published δ¹¹B-derived pH_{sw} records provide decadal to centennial timescales records^{16,17}. The two records from Flinders¹⁶ and Arlington Reefs¹⁷ of the Great Barrier Reef (GBR) (Fig. 1) express a signature of pH_{sw} reduction over the last 50 years. However, the inconsistency of pH_{sw} variations during AD 1800–2000 for the two records (Supplementary Fig. 4) cannot provide convincing evidence for a decrease in pH_{sw} that can be unambiguously attributed to atmospheric CO₂ rising.

In this study, we present a new pH_{sw} record inferred from skeletal δ¹¹B data of modern and fossil corals from Xiaodonghai Reef (18°12.46'N, 109°29.93'E), located in the South China Sea (SCS) (Fig. 1). The modern coral record spans from AD 1838–2001, before the beginning of the Industrialization Period and covers the current

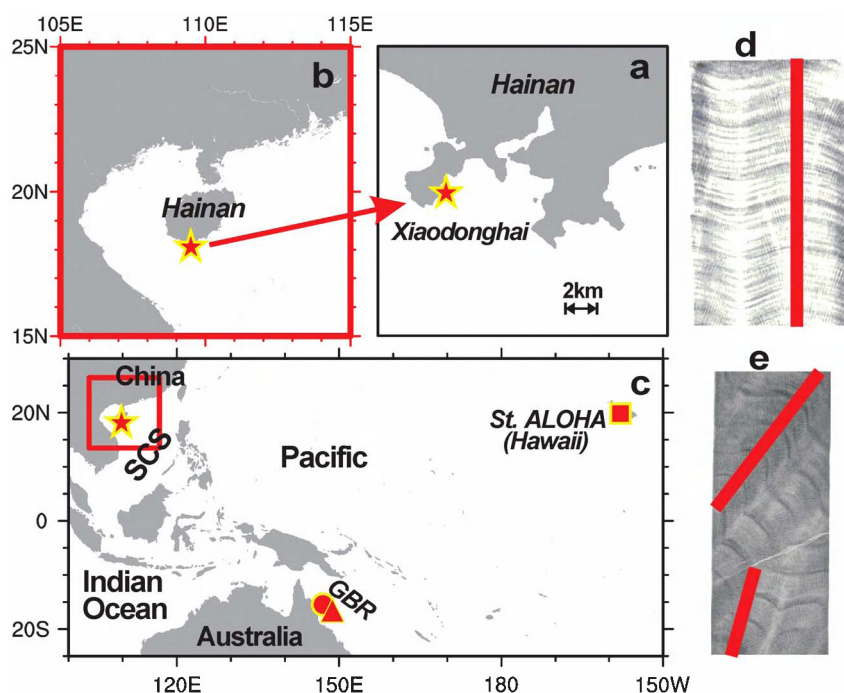


Figure 1 | Maps with study sites. Modern and fossil *Porites* cores were drilled from (a) Xiaodonghai Reef (star), located off (b) southern Hainan in (c) the northern South China Sea (SCS). Circle, triangle and square symbols denote the locations of Arlington Reef¹⁷ and Flinders Reef⁶ in the Great Barrier Reef (GBR) and Station of ALOHA⁹ in Hawaii, respectively. The maps created using NCAR Command Language (<http://www.ncl.ucar.edu/>) and MapPlot the Earth.4 dataset (http://www.ncl.ucar.edu/Document/HLUs/Classes/MapPlotData4_1_earth_4.shtml). Representative X-radiographs of slices of (d) modern coral sample Song-5 and (e) fossil coral sample Dong-5 are also shown. Red lines denote the subsampling transect along the maximum growth axis.

warm period (CWP, since 1950s). The $\delta^{11}\text{B}$ -inferred record of a precisely ^{230}Th -dated¹⁸ fossil coral records values from AD 1048–1079, within the Medieval Warm Period (MWP)¹⁹. Understanding pH_{sw} variations in the MWP of the last millennium without anthropogenic CO_2 perturbation will be helpful in understanding modern acidification in the CWP.

Results

Measured $\delta^{11}\text{B}$ values of modern and fossil corals are given in Supplementary Figure 3 and Supplementary Tables 2–4. The pH_{sw} values (total scale) were calculated from measured $\delta^{11}\text{B}$ data (see Methods and ref. 15). The coral-reconstructed pH_{sw} record from AD 1838–2001 varies from 7.82 to 8.21 (Fig. 2b). There is a ~30-yr period with maximal pH_{sw} values of 8.20–8.21 during AD 1830–1870. A minimum pH_{sw} value of 7.82 occurred from AD 1990–1993. Striking features of this record includes a decreasing trend of $-0.0015 \pm 0.0002 \text{ pH year}^{-1}$ from AD 1838–2001 ($R^2 = 0.63$, $p < 0.0001$) and inter-decadal variations with amplitudes of 0.1–0.2 units (Fig. 2b). The reconstructed bi-weekly pH_{sw} data in AD 2000 displays strong seasonality, from high values of ~8.1 in winter to low values of ~7.6 in summer (Fig. 3b). This seasonal pH_{sw} change is consistent with local instrumental data (Supplementary Fig. 7), and follows intra-annual seawater pCO_2 variations of SCS reef water, from a high value of ~500 μatm in summer to a low value of ~380 μatm in winter^{20,21}. A 32-yr fossil coral-derived pH_{sw} record is characterized by a high average value of 8.17 ± 0.08 (2σ , $n = 8$) (Fig. 2c).

Discussion

The longest *in-situ* pH_{sw} record at Station ALOHA in Hawaii shows a significant decreasing trend of $-0.018 \text{ pH year}^{-1}$ in surface water of the central North Pacific Ocean over the past two decades (AD 1988–2011) (Supplementary Fig. 4)⁹. Our coral-inferred pH_{sw} reconstruction from the SCS provides the first evidence of a decreasing trend,

traced back to the Industrialization Period (Fig. 2b). Atmospheric CO_2 increased slightly between AD 1840 and 1950 at a rate of $0.270 \pm 0.010 \text{ ppm year}^{-1}$ ($R^2 = 0.97$, $p < 0.0001$), after which the rate increases dramatically to $1.135 \pm 0.062 \text{ ppm year}^{-1}$ ($R^2 = 0.97$, $p < 0.0001$) (Fig. 2). Our pH_{sw} sequence follows the temporal pattern of CO_2 . The coral-inferred pH_{sw} values of 8.1–8.2 in AD 1830–1870 are not significantly different from those in the MWP (Fig. 2). The values decreased at a rate of $-0.0011 \pm 0.0003 \text{ pH year}^{-1}$ ($R^2 = 0.35$, $p = 0.0009$) in a 110-yr interval after AD 1840. This rate of decline almost tripled to $-0.0029 \pm 0.0013 \text{ pH year}^{-1}$ ($R^2 = 0.33$, $p = 0.04$) after AD 1950. This pH_{sw} follows changes observed in the CO_2 time series (Pearson correlation coefficient: $R^2 = 0.63$, $n = 41$, $p < 0.0001$). The long-term decreasing trend of pH_{sw} also corresponds to a shift to more negative $\delta^{13}\text{C}$ values ($-0.0037 \pm 0.0010 \text{ year}^{-1}$, $R^2 = 0.26$, $p = 0.0007$, AD 1838–2001) (Supplementary Fig. 5b), where a significant positive correlation ($R^2 = 0.21$, $n = 41$, $p = 0.003$) exists between pH_{sw} and $\delta^{13}\text{C}$. This suggests synchronous changes between seawater acidification and decreasing dissolved inorganic carbon (DIC) in this region. The $\delta^{13}\text{C}$ change could be attributed to the “Suess effect”, which is due to uptake of atmospheric CO_2 by the oceans that has been progressively depleted in ^{13}C by combustion of fossil fuels, as supported by previous studies^{16,17}. These signatures all reflect the remarkable absorption of anthropogenic CO_2 by the ocean, and induced acidification in response to the rapid rise in atmospheric CO_2 since the Industrialization Period.

While atmospheric CO_2 governs the long-term SCS pH_{sw} trend, the inter-decadal cycles of 0.1–0.2 pH must be linked to other mechanism, in the absence of significant inter-decadal variability in atmospheric CO_2 . The physical-biogeochemical conditions of the SCS are strongly influenced by the Asian monsoon^{22,23}. During summer, this region is affected by the southwest Asian summer monsoon (ASM), which brings warm and wet tropical air masses to the study area, resulting in increased precipitation (Supplementary Fig. 1b). However there is no correlation between the coral-inferred pH_{sw}

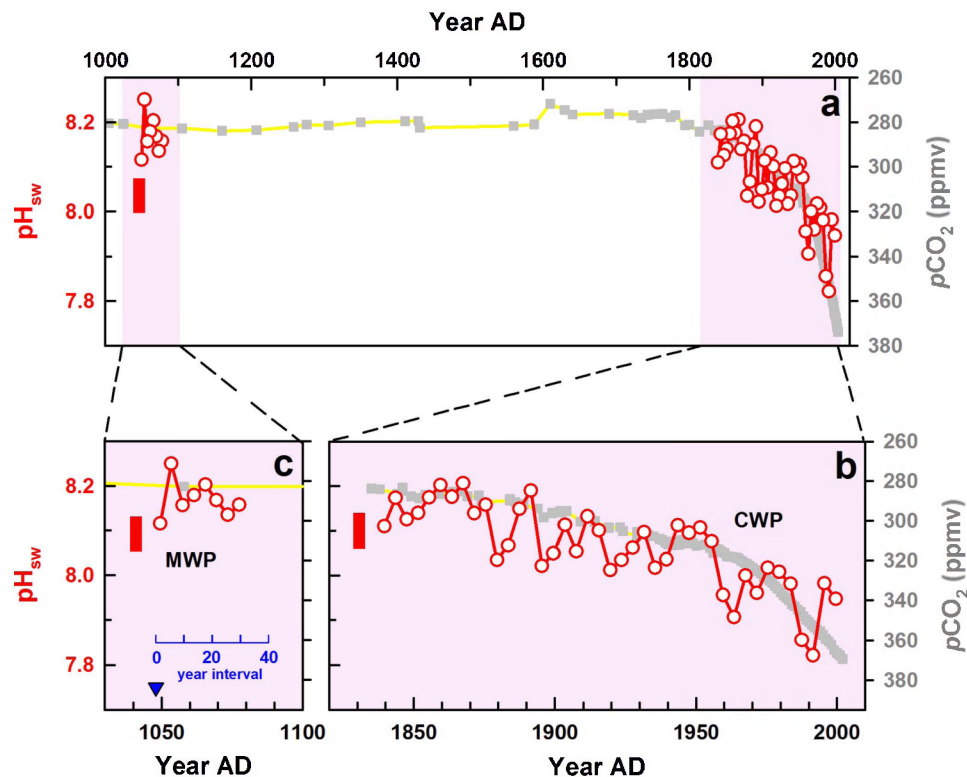


Figure 2 | Coral-inferred pH_{sw} in the SCS and atmospheric CO_2 (ref. 32). Comparison of the pH_{sw} (red circles and lines) based on boron isotope and atmospheric CO_2 (gray dots and yellow line) from (a) AD 1000–2000 and two enlarged sections during (b) AD 1030–1100 and (c) AD 1830–2001. CO_2 data after 1958 (included) are annual averages of direct observations from Mauna Loa and the South Pole³². CO_2 data before 1958 are from ice cores³³. Vertical red bars denote the 2σ uncertainty of pH_{sw} . Dark blue triangle in (c) indicates position of ^{230}Th -dated layer. The chronology of fossil sample was set by year intervals relative to the dating layer.

and the precipitation record (Supplementary Fig. 6). The Asian winter monsoon (AWM) prevails during November to March, bringing cold and dry continental air associated with the Siberian High. From AD 1994 to 2011, the monthly mean wind speed varied from 0.4 to 11 m s^{-1} , with prominent peaks occurring during the winter monsoon season (Supplementary Fig. 1c). We found a significant correlation ($R^2 = 0.20$, $n = 41$, $p = 0.003$) between the pH_{sw} and Siberian High pressure, an index of AWM intensity²⁴. Low and high pH_{sw} values respectively co-vary with weak and strong Siberian High phases on an inter-decadal timescale (Fig. 3c). It is a robust feature that the significant correlation ($R^2 = 0.18$, $n = 41$, $p = 0.006$) still exists for the two detrended sequences (Fig. 3d). This concurrence suggests that the AWM may contribute to changes in regional pH_{sw} in the SCS.

The linkage between pH_{sw} and AWM is attributable to the flushing efficiency of waters over the reefs as observed in the GBR¹⁶ and monsoon-driven productivity. During weak AWM periods with reduced wind forcing²² in the SCS, the build-up of CO_2 due to calcification and respiration could lower pH_{sw} due to poor flushing of reef waters by open seawater. In contrast, periods of relatively strong AWM with strengthened surface currents²² could result in higher pH_{sw} values. At the same time, surface primary productivity of the SCS is also controlled by AWM intensity²³. A weak (strong) AWM would cause the nutricline to deepen (shallow) and result in lower (higher) surface productivity²³ and decreased (increased) pH_{sw} . This mechanism is strongly supported by the co-variation of biweekly-resolved coral-inferred pH_{sw} and AWM wind speed data from AD 2000 (Fig. 3b).

The most acidic condition in AD 1990 is coincident with a sharp drop in the Siberian High index (Fig. 3c), an unprecedented weak event during the past four centuries²⁴. Global warming preferentially

warms the high latitudes of Eurasia and this decreases the land-sea pressure gradient and weakens the AWM²⁵. The expected rise in atmospheric CO_2 will likely reduce the AWM intensity in the coming decades²⁵ and exacerbate the impact of acidification on the SCS, and threaten the most diverse collection of shallow water marine organisms on Earth²⁶. Under the stress of current accelerated ocean acidification, an in-depth understanding of the ecological and socioeconomic repercussions in the SCS and other monsoon regions is imperative.

Methods

Coral cores. A 3-m long core of *Porites* sp. coral, Song-5, was drilled from Xiaodonghai Reef ($18^\circ 12.46' \text{N}$, $109^\circ 29.93' \text{E}$), at a water depth of 8.5 m offshore south Hainan in April 2002 (Fig. 1). Slabs, 7 mm in thickness, were sectioned, washed with ultrapure water, and then dried for X-ray images. Annual banding counts were used to establish the chronology. Subsamples were milled in continuous 4-yr intervals down the full length of the core along the maximum growth axis for the period AD 1838 to 2001. A set of biweekly resolution subsamples was milled from the AD 2000 segment. One more 1-m long core fossil *Porites* sp. coral, Dong-5, was also drilled. Subsamples were milled at 4-year intervals along the maximum growth axis on a 32-yr section. X-ray diffraction analysis shows coral samples are 100% aragonite and scanning electron microscopy image indicates an absence of secondary aragonite. After ground into a homogeneous powder using a pre-cleaned agate, all the subsamples (1–3 mg) were treated with 10% NaOCl and ultrapure water (18.2 M Ω) in an ultrasonic bath.

Isotopic analysis and dating. Micro-sublimation techniques were used for boron purification²⁷. Aliquots (~50 μL) containing 50–100 ng of boron were then diluted to 20 ppb boron for the isotopic measurements. $\delta^{11}\text{B}$ compositions were determined by a multi-collector inductively coupled plasma mass spectrometer (MC-ICP-MS), Thermo Neptune, at the Earth Dynamic System Research Center, National Cheng Kung University. Instrumental mass bias was calibrated using standard-sample bracketing techniques^{27,28} with NIST SRM 951 boric acid. At each analytical sequence, two JCP-1 and JCT-1 carbonate standards (*Porites* sp. and giant clam Geological Survey of Japan) and one in-house standard Alfa-B (B ICP-MS solution, Alfa Aesar) were used to monitor the micro-sublimation procedure and plasma condition in

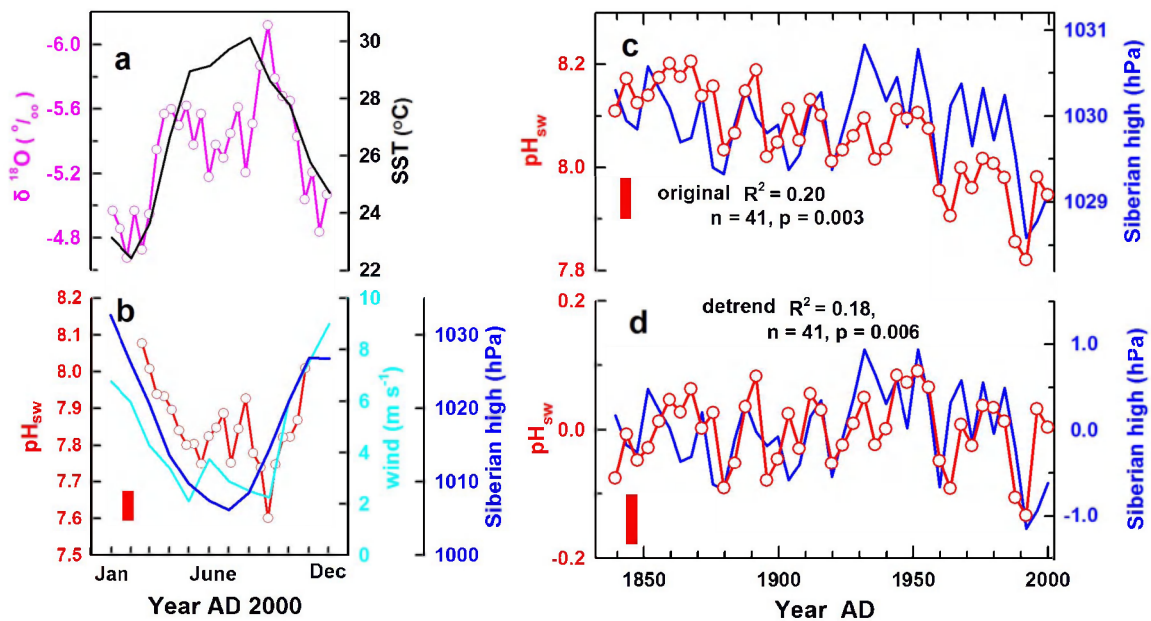


Figure 3 | Biweekly-resolution coral data and environmental parameters in AD 2000 and time series of the reconstructed pH_{sw} based on boron isotope and Siberian High index²⁴ from AD 1838–2001. (a) Coral $\delta^{18}\text{O}$ (pink) and sea surface temperature (SST) (black line), and (b) coral-inferred pH_{sw} (red), wind speed (cyan line) and Siberian High index²⁴ (blue line) in AD 2000. Monthly SST data (17–19°N, 115–117°E) with a 1° resolution were from the Optimum Interpolation Sea Surface Temperature, Version 2, National Oceanic and Atmospheric Administration (NOAA): (<http://www.esrl.noaa.gov/psd/data/gridded/data.noaa.oisst.v2.html>). Wind data (17–19°N, 115–117°E) with a 0.25° resolution were from the Blended Sea Winds provided by the NOAA National Climate Data Center: (<http://www.ncdc.noaa.gov/oa/rsad/air-sea/seawinds.html>). Intra-annual data were calendared by aligning coral $\delta^{18}\text{O}$ maxima with SST minima and applying a linear interpolation between anchor points. (c) Comparison of coral-inferred pH_{sw} data and 4-yr averaged Siberian High index²⁴ (blue line), and (d) detrended pH_{sw} data and Siberian High index. Vertical red bars denote the 2σ uncertainty of pH_{sw} .

order to maintain analytical accuracy. The JCP-1 and JCT-1 standard yielded a mean value of $24.20 \pm 0.24\%$ (2σ , $n = 9$) and $16.21 \pm 0.05\%$ (2σ , $n = 3$) respectively. The external precision of $\delta^{11}\text{B}$ measurements are better than $\pm 0.28\%$ (2σ)²⁷. The procedure blank is < 5 pg of boron. Instrument sensitivity for 20 ppb B was 0.4–0.5 V for ^{11}B signal intensity, and the effect of total blanks (< 0.01 V, including procedure blank and instrument background) can be negligible. Boron isotopic ratios are expressed using delta (δ) notation relative to the NIST SRM 951. The $\delta^{13}\text{C}$ and $\delta^{18}\text{O}$ measurements were carried out using an isotope ratio mass spectrometer MAT-252 equipped with a micro carbonate automatic sample input Kiel II device in the Institute of Earth Environment, Chinese Academy of Sciences. Results are expressed using delta (δ) notation relative to the Vienna Pee Dee Belemnite (V-PDB) standard. The external error of the laboratory standard is $\pm 0.1\%$ and $\pm 0.2\%$ (1σ) for $\delta^{13}\text{C}$ and $\delta^{18}\text{O}$, respectively.

The fossil coral 5 Dong was dated by ^{230}Th techniques¹⁸ (Supplementary Table 1) by a MC-ICP-MS, Thermo Neptune, at the High-Precision Mass Spectrometry and Environment Change Laboratory (HISPEC), National Taiwan University. The first annual banding of the 32-yr section was sampled for dating.

pH calculation. The pH_{cf} was converted by boron isotope systematics based on a following equation²⁹:

$$\text{pH}_{\text{cf}} - \text{p}K_{\text{B}} - \log \left\{ \frac{[\delta^{11}\text{B}_{\text{sw}} - \delta^{11}\text{B}_{\text{coral}}] / [\alpha_{(\text{B}_3 - \text{B}_4)} \delta^{11}\text{B}_{\text{coral}} - \delta^{11}\text{B}_{\text{sw}} - 1000(\alpha_{(\text{B}_3 - \text{B}_4)} - 1)]}{\alpha_{(\text{B}_3 - \text{B}_4)}} \right\},$$

where $\delta^{11}\text{B}_{\text{sw}}$ and $\delta^{11}\text{B}_{\text{coral}}$ represents $\delta^{11}\text{B}$ in seawater ($\delta^{11}\text{B}_{\text{sw}} = 39.5\%$)²⁸ and in coral, respectively, and $\alpha_{(\text{B}_3 - \text{B}_4)} = 1.0272$ (ref. 30). The dissociation constant of boric acid $\text{p}K_{\text{B}}$ is 8.597 at 25 °C and a salinity of 35 (ref. 31). The pH_{sw} value was calculated using the empirical equation: $[\text{pH}_{\text{sw}} = (\text{pH}_{\text{cf}} - 4.72)/0.466]$, $R^2 = 0.99$ (refs. 14,15). The external uncertainty of $\pm 0.28\%$ (2σ) (ref. 27) for $\delta^{11}\text{B}$ data corresponds to a precision of better than ± 0.02 units for pH_{cf} and ± 0.04 for pH_{sw} . The biweekly pH_{sw} was corrected by temperature effect³¹ on $\text{p}K_{\text{B}}$.

- Hönisch, B., Hemming, N. G., Archer, D., Siddall, M. & McManus, J. F. Atmospheric carbon dioxide concentration across the Mid-Pleistocene Transition. *Science* **324**, 1551–1554 (2009).
- Sabine, C. L. *et al.* The oceanic sink for anthropogenic CO_2 . *Science* **305**, 367–371 (2004).
- Brewer, P. G. A changing ocean seen with clarity. *Proc. Natl. Acad. Sci. USA* **106**, 12213–12214 (2009).

- Caldeira, K. & Wickett, M. E. Anthropogenic carbon and ocean pH. *Nature* **425**, 365 (2003).
- Orr, J. C. *et al.* Anthropogenic ocean acidification over the twenty-first century and its impact on calcifying organisms. *Nature* **437**, 681–686 (2005).
- Hoegh-Guldberg, O. *et al.* Coral reefs under rapid climate change and ocean acidification. *Science* **318**, 1737–1742 (2007).
- Pandolfi, J. M., Connolly, S. R., Marshall, D. & Cohen, A. L. Projecting coral reef futures under global warming and ocean acidification. *Science* **333**, 418–422 (2011).
- Inoue, S., Kayanne, H., Yamamoto, S. & Kurihara, H. Spatial community shift from hard to soft corals in acidified water. *Nature Clim. Change* **3**, 683–687 (2013).
- Dore, J. E., Lukas, R., Sadler, D. W., Church, M. J. & Karl, D. M. Physical and biogeochemical modulation of ocean acidification in the central North Pacific. *Proc. Natl. Acad. Sci. USA* **106**, 12235–12240 (2009).
- Byrne, R. H., Mecking, S., Feely, R. A. & Liu, X. Direct observations of basin-wide acidification of the North Pacific Ocean. *Geophys. Res. Lett.* **37**, L02601; DOI: 10.1029/2009GL040999 (2010).
- Vengosh, A., Kolodny, Y., Starinsky, A., Chivas, A. R. & McCulloch, M. T. Coprecipitation and isotopic fractionation of boron in modern biogenic carbonates. *Geochim. Cosmochim. Acta* **55**, 2901–2910 (1991).
- Hemming, N. G. & Hanson, G. N. Boron isotopic composition and concentration in modern marine carbonates. *Geochim. Cosmochim. Acta* **56**, 537–543 (1992).
- Al-Horani, F. A., Al-Moghrabi, S. M. & de Beer, D. The mechanism of calcification and its relation to photosynthesis and respiration in the scleractinian coral *Galaxea fascicularis*. *Mar. Biol.* **142**, 419–426 (2003).
- Trotter, J. *et al.* Quantifying the pH ‘vital effect’ in the temperate zooxanthellate coral *Cladocora caespitosa*: Validation of the boron seawater pH proxy. *Earth Planet. Sci. Lett.* **303**, 163–173 (2011).
- McCulloch, M. T., Falter, J., Trotter, J. & Montagna, P. Coral resilience to ocean acidification and global warming through pH up-regulation. *Nature Clim. Change* **2**, 623–627 (2012).
- Pelejero, C. *et al.* Preindustrial to modern interdecadal variability in coral reef pH. *Science* **309**, 2204–2207 (2005).
- Wei, G., McCulloch, M. T., Mortimer, G., Deng, W. & Xie, L. Evidence for ocean acidification in the Great Barrier Reef of Australia. *Geochim. Cosmochim. Acta* **73**, 2332–2346 (2009).
- Shen, C.-C. *et al.* High-precision and high-resolution carbonate ^{230}Th dating by MC-ICP-MS with SEM protocols. *Geochim. Cosmochim. Acta* **99**, 71–86 (2012).
- Moinuddin, A. *et al.* Continental-scale temperature variability during the past two millennia. *Nature Geosci.* **6**, 339–346 (2013).



20. Dai, M. *et al.* Diurnal variations of surface seawater $p\text{CO}_2$ in contrasting coastal environments. *Limnol. Oceanogr.* **54**, 735–745 (2009).
21. Yan, H. *et al.* Coral reef ecosystems in the South China Sea as a source of atmospheric CO_2 in summer. *Chinese Sci. Bull.* **56**, 676–684 (2011).
22. Xu, D. & Malanotte-Rizzoli, P. The seasonal variation of the upper layers of the South China Sea (SCS) Circulation and the Indonesian through flow (ITF): An ocean model study. *Dynam. Atmos. Oceans* **63**, 103–130 (2013).
23. Liu, K.-K. *et al.* Inter-annual variation of chlorophyll in the northern South China Sea observed at the SEATS Station and its asymmetric responses to climate oscillation. *Biogeosciences Discuss.* **10**, 6899–6938 (2013).
24. D'Arrigo, R., Wilson, R., Panagiotopoulos, F. & Wu, B. On the long-term interannual variability of the East Asian winter monsoon. *Geophys. Res. Lett.* **32**, L21706; DOI: 10.1029/2005GL023235 (2005).
25. Hori, M. E. & Ueda, H. Impact of global warming on the East Asian winter monsoon as revealed by nine coupled atmosphere-ocean GCMs. *Geophys. Res. Lett.* **33**, L03713; DOI: 10.1029/2005GL024961 (2006).
26. Morton, B. & Blackmore, G. South China Sea. *Mar. Pollut. Bull.* **12**, 1236–1263 (2001).
27. Wang, B.-S. *et al.* Direct separation of boron from Na- and Ca-rich matrices by sublimation for stable isotope measurement by MC-ICP-MS. *Talanta* **82**, 1378–1384 (2010).
28. Foster, G. L. Seawater pH, $p\text{CO}_2$ and $[\text{CO}_3^{2-}]$ variations in the Caribbean Sea over the last 130 kyr: A boron isotope and B/Ca study of planktic foraminifera. *Earth Planet. Sci. Lett.* **271**, 254–266 (2008).
29. Zeebe, R. E., Sanyal, A., Ortiz, J. D. & Wolf-Gladrow, D. A. A theoretical study of the kinetics of the boric acid-borate equilibrium in seawater. *Mar. Chem.* **73**, 113–124 (2001).
30. Klochko, K., Kaufman, A. J., Yao, W., Byrne, R. H. & Tossell, J. A. Experimental measurement of boron isotope fractionation in seawater. *Earth Planet. Sci. Lett.* **248**, 276–285 (2006).
31. Dickson, A. G. Thermodynamics of the dissociation of boric acid in synthetic seawater from 273.15 to 318.15 K. *Deep Sea Res. Part A* **37**, 755–766 (1990).
32. Keeling, C. D. *et al.* Atmospheric CO_2 and $^{13}\text{CO}_2$ exchange with the terrestrial biosphere and oceans from 1978 to 2000: observations and carbon cycle implications. In *A History of Atmospheric CO_2 and its effects on Plants, Animals, and Ecosystems*. (Eds Ehleringer, J. R. *et al.*) 83–113 (Springer Verlag, New York, 2005).
33. Meure, M. C. *et al.* Law Dome CO_2 , CH_4 and N_2O ice core records extended to 2000 years BP. *Geophys. Res. Lett.* **33**, L14810; DOI: 10.1029/2006GL026152 (2006).

Acknowledgments

This study was jointly supported by National Key Basic Research Program of China (2013CB956102 to Y.L.), Strategic Priority Research Program of the CAS (XDA05080300 to K.F.Y.), National Science Foundation of China (41003002 to Y.L.), NSC and MOE Top University Program (120-2116-M006-006 to C.F.Y.), MOST and NTU grants (101-2116-M-002-009, 102-2116-M-002-016, and 101R7625 to C.C.S.).

Author contributions

Y.L., Z.P. and C.-F.Y. designed and initiated the research. Y.L., Y.-B.L. and C.-F.Y. analyzed B isotope. S.S. and L.X. drilled the cores. C.-C.W. and C.-C.S. conducted ^{230}Th dating. W.L. analyzed O and C isotopes. R.Z., C.-F.Y., K.Y., G.W. and G.B. contributed significantly to the discussion of results and manuscript. Y.L. and C.-C.S. wrote the paper.

Additional information

Supplementary information accompanies this paper at <http://www.nature.com/scientificreports>

Competing financial interests: The authors declare no competing financial interests.

How to cite this article: Liu, Y. *et al.* Acceleration of modern acidification in the South China Sea driven by anthropogenic CO_2 . *Sci. Rep.* **4**, 5148; DOI:10.1038/srep05148 (2014).



This work is licensed under a Creative Commons Attribution-NonCommercial-ShareAlike 3.0 Unported License. The images in this article are included in the article's Creative Commons license, unless indicated otherwise in the image credit; if the image is not included under the Creative Commons license, users will need to obtain permission from the license holder in order to reproduce the image. To view a copy of this license, visit <http://creativecommons.org/licenses/by-nc-sa/3.0/>